

Phosphorylation as a Method of Tuning the Enantiodiscrimination Potency of Quinine—An NMR Study

LUKASZ GÓRECKI,¹ LUKASZ BERLICKI,¹ ARTUR MUCHA,¹ PAWEŁ KAFARSKI,¹ KATARZYNA ŚLEPOKURA,² AND EWA RUDZIŃSKA-SZOSTAK^{1*}

¹Department of Bioorganic Chemistry, Faculty of Chemistry, Wrocław University of Technology, Wrocław, Poland

²Faculty of Chemistry, University of Wrocław, Wrocław, Poland

ABSTRACT Quinines phosphorylated at the C-9 hydroxyl group (diphenyl and diethyl phosphates) were synthesized and validated as novel effective chiral solvating agents in two alternative methods based on ¹H and ³¹P NMR spectroscopy. Tested with a representative set of racemic analytes, the title compounds induced shift nonequivalence effects in ¹H NMR signals with values up to 0.1–0.2 ppm for 3,5-dinitrobenzoyl-substituted amino acids. In terms of enantiodifferentiation extent and application range, introduction of a phosphate group was proven to be superior compared to the action of nonmodified quinine. Interestingly, a temperature decrease to reach the slow exchange conditions also produced nonequivalences in the ³¹P NMR spectra of the selectors. Comprehensive NMR analysis showed the existence of two conformations (closed 1 and 2) for both quinines in their free forms and the open 3 arrangement for the protonated ones. The crystal structure of diethylphosphorylquinine hydrochloride dichloromethane hemisolvate revealed a similar conformation to that observed in solution. Structures of complexes of phosphorylated quinines with selected ligands were determined with the use of NMR-based molecular modeling studies. *Chirality* 24:318–328, 2012. © 2012 Wiley Periodicals, Inc.

KEY WORDS: alkaloids; phosphorylation; conformation analysis; chiral auxiliaries; NMR spectroscopy

INTRODUCTION

Quinine, the major component of *Cinchona* alkaloids, represents one of the most privileged molecules exploited in chiral recognition applications.¹ Its structural arrangement involves the simultaneous presence of a methoxy-substituted quinoline system and constrained bicyclic vinyl-substituted quinuclidine tertiary amine system, all connected by a hydroxymethylene linker. The unique three-dimensional assembly of quinine is emphasized by the presence of four carbon and one nitrogen stereogenic centers. These features together with multifunctional heteroatom variety offer different kinds of potentially stereoselective contacts, including ion pairing, hydrogen bonding, dipole–dipole, π – π and van der Waals interactions. The chiral recognition demonstrated by quinine, influenced by additional conformational factors, has been the matter of numerous theoretical and spectroscopic investigations (for representative recent examples, see Refs. 2–7). As a consequence, quinine- and quinine-based chiral auxiliaries and catalyst components have been successfully employed in asymmetric synthesis.^{1,8} Stereoselective techniques of analysis and the separation of enantiomers represent additional subjects of great interest in this field. Appropriate derivatives have served as chiral stationary phases in HPLC or CEC^{9–12} or background electrolyte additives in nonaqueous CE.¹³ Finally, they have been found to be chiral solvating agents (CSAs) in the NMR determination of the enantiomeric composition of various analytes.

The formation of dynamic diastereomeric solvates with quinine produces diagnostic nonequivalences in different enantiotopic nuclei. Accordingly, selected proton and fluorine resonances were indicative of enantiomers of substituted

binaphthyl compounds, alkylarylcarbinols and others in the original works of Salvadori et al.^{14,15} Being inexpensive and soluble in standard NMR solvents, nonderivatized quinine has been applied for the characterization of composition of compounds and the enantioselectivity of selected reactions, mainly those involving hydroxyl derivatives. Thus, ¹H NMR has served to determine the optical purity of secondary alcohols obtained through the enantioselective addition of diethylzinc to furfuraldehydes,¹⁶ as well as for the analysis of β -hydroxy esters¹⁷ and cyclic hemiacetals and methyl acetals.¹⁸ Secondary and tertiary α -aryl- α -trifluoromethyl alcohols and hydroxyesters were studied by the use ¹⁹F NMR,¹⁹ whereas ³¹P NMR allowed enantiodiscrimination of 1-hydroxy,²⁰ 1,2-dihydroxyalkanephosphonates²¹ and *N*-benzyloxycarbonylamino-phosphonates²² in our group. Triphenyltin-modified alcohols and acids showed chemical shift anisochrony in ¹¹⁹Sn NMR.²³ The encouraging results of these applications induced further attempts to modify the fundamental quinine structure, preferentially at the C9 and C11 positions. Consistent with their successful chromatographic utility, C9-carbamoylated derivatives were tested as CSAs against a range

This article is dedicated to Prof. Francisco Palacios on the occasion of his 60th anniversary.

Additional Supporting Information may be found in the online version of this article.

Contract grant sponsor: The work was financed by a statutory activity subsidy from the Polish Ministry of Science and Higher Education for the Faculty of Chemistry of Wrocław University of Technology.

*Correspondence to: Ewa Rudzińska-Szostak, Department of Bioorganic Chemistry, Faculty of Chemistry, Wrocław University of Technology, Wyb. rzeże Wyspiańskiego 27, Wrocław 50-370, Poland.

E-mail: ewa.rudzinska@pwr.wroc.pl

Received for publication 28 September 2011; Accepted 14 December 2011

DOI: 10.1002/chir.22000

Published online 17 February 2012 in Wiley Online Library (wileyonlinelibrary.com).

chiral substrates, including amines, acids, amides and *N*-protected amino acids.^{24–27} Additionally, penta- and hexavalent organophosphorus species have been found to be important structural elements of synthetic receptors.^{28,29} In particular, thiophosphonates,^{30,31} 1,1'-dinaphthyl-2,2'-diylphosphoric acid^{32,33} and dianaphthyl- and/or *o*-cresol-derived hexacoordinated phosphates^{34,35} are effective CSAs in NMR spectroscopy. Importantly, the synthetic availability of such compounds should not be a limiting aspect of their applications.

In this work, a combination of an easily available, unique chiral scaffold of quinine with a phosphate moiety that shows good complexing properties toward different ligands was investigated. We explore a novel, synthetically feasible way of derivatizing the C9 hydroxyl and evaluate its influence on the enantiodiscrimination effect. The functionalization led to phosphorylated quinines that could offer new potential interactions with analytes via oxygen atom-rich moieties. The modified compounds were subsequently validated as CSAs in ¹H NMR spectroscopy under fast exchange conditions against a collection of model chiral selectands. Using the characteristic features of the selector, the recognition phenomenon was additionally studied by means of ³¹P NMR at low temperature to reach slow exchange conditions. Detailed conformational analysis of phosphorylated quinine in the free form, protonated and complexed with a selected ligands was performed with the use of the NMR and molecular modeling techniques.

MATERIALS AND METHODS

General

All solvents and reagents purchased from commercial suppliers (Aldrich, Sigma, Merck, POCh, Armar) were of analytical grade and were used without further purification. High resolution mass spectra were measured on an LCT Premier XE (Waters) apparatus with electrospray ionization (positive ion mode). NMR experiments were performed on a Bruker AvanceTM 600 MHz.

NMR Measurements

Measurements at 298, 293, 283, and 250 K were made in CDCl₃ solution. To improve the solubility of ligands **3a**, **3b**, and **3c**, 2, 4, and 6% DMSO were added to the CDCl₃ solutions, respectively. Measurements at 180 and 200 K were performed in CD₂Cl₂. The signal assignment of the ¹H spectra of receptors **1** and **2b**, their hydrochloride salts and their 1:1 complexes with **S-3b** at 50 mM in CDCl₃ at 298 K and 10 mM in CD₂Cl₂ at 200 K was assisted by ¹H-¹H COSY, ROESY and ¹H-¹³C HSQC spectra. Typical 1D and 2D ROESY spectra were recorded in phase-sensitive mode by employing a spin lock of 0.1 s at 200 K and 0.1–1.2 s at 298 K. Coupling constants were determined from ¹H inverse gated decoupled ³¹P spectra.

Crystal Structure

The crystallographic measurement for **2b** hydrochloride dichloromethane hemisolvate (**2b**×HCl×0.5CH₂Cl₂; colorless; 0.35 × 0.10 × 0.07 mm³) was performed on a Xcalibur PX automated four-circle diffractometer with the graphite-monochromatized Mo-K_α radiation at 100(2) K. Data collection, cell refinement, and data reduction and analysis were carried out with CrysAlisCCD and CrysAlisRED, respectively.³⁶ Analytical absorption correction was applied to the data with the use of CrysAlisRED. The structure was solved by direct methods using SHELXS-97,³⁷ and refined on *F*² by a full-matrix least-squares technique using SHELXL-97³⁷ with anisotropic thermal parameters for non-H atoms. Dichloromethane molecule lies on a twofold axis and therefore its s.o.f. is 0.5. All H atoms were found in difference Fourier maps. In the final refinement cycles, they were treated as riding atoms in geometrically optimized positions, with N–H = 0.93 Å and C–H = 0.95–1.00 Å, and with *U*_{iso}(H) = 1.2*U*_{eq}(N,C) for NH, CH and CH₂, or 1.5*U*_{eq}(C) for CH₃.

The figure was made using an XP program.³⁸ Crystal data for **2b**×HCl×0.5CH₂Cl₂: C_{24.5}H₃₅Cl₂N₂O₅P, *M* = 539.41, orthorhombic, space group *P*2₁2₁2, *a* = 11.868(4), *b* = 28.248(9), *c* = 7.999(3) Å, *V* = 2681.6(16) Å³, *Z* = 4, *T* = 100(2) K, *μ* = 0.34 mm⁻¹, analytical absorption correction (*T*_{min} = 0.957, *T*_{max} = 0.978), 20,122 measured reflections, 7428 independent refl., 3529 reflections with *I* > 2σ(*I*), *θ*_{min} = 2.76°, *θ*_{max} = 30.07°, *R*₁ = 0.048, *wR*₂ (all data) = 0.052, Δρ (max/min) = 0.39/–0.46 eÅ⁻³. CCDC-831387 contains the supplementary crystallographic data for this article. These data can be obtained free of charge from The Cambridge Crystallographic Data Centre via www.ccdc.cam.ac.uk/data_request/cif.

Molecular Modeling

All calculations were performed with the use of Discovery Studio v 2.5 (Accelrys). Optimizations were conducted with application of the CHARMM forcefield, the Momany-Rone method of atom partial charge computation, the Smart Minimizer algorithm, and up to an RMS gradient 0.01 Å. Minimizations were performed in two steps: (a) with the constraints obtained from NMR measurements and (b) without any constraints.

Chemistry

Ligands **3g-n** are commercially available (Aldrich). Racemic compounds **3a-f** were synthesized according to the standard methods.³⁹ Enantiomerically pure **3a** and **3b** were obtained using the method published by Pirkle.⁴⁰ The monochloride of nonmodified quinine and the phosphorylated quinines were prepared by the addition of an equivalent amount of methanolic hydrogen chloride to the free amine followed by solvent evaporation.

General Procedure of Phosphorylation

t-BuOK (10.2 mmol, 1.145 g) was added in one portion to a solution of quinine (10 mmol, 3.244 g) in dry tetrahydrofuran (100 ml) and then cooled to –78°C. After 0.5 h, diethyl chlorophosphate (10.5 mmol, 1.812 g) or diphenyl chlorophosphate (10.5 mmol, 2.821 g) dissolved in 3 ml of THF was added dropwise to the reaction mixture. Stirring was continued for 2 h at –78°C and overnight at room temperature. The volatile components were evaporated under reduced pressure, and the residue was dissolved in ethyl acetate, washed with water and dried over MgSO₄. The solvent was removed on a rotary evaporator, and the final product was purified via column chromatography using silica gel and an ethyl acetate/methanol mixture (4:1) as the eluent. The solvents were removed from the collected fractions, and the residue was treated with diethyl ether and stored in the fridge for crystallization. The resulting phosphorylated quinine was filtered after a few days.

9-*O*-Diphenylphosphorylquinine (**2a**)

Colorless crystals, yield 66%, m.p. 97.5–98.5°C. HRMS (TOF MS ESI): *m/z* calcd for C₃₂H₃₄N₂O₅P⁺: 557.2205 [*M*+H]⁺; found: 557.2193. ¹H NMR (600 MHz, CDCl₃, 25°C): δ (ppm) 8.68 (d, ³*J*_{H,H} = 4.5 Hz, 1H; H-2), 8.01 (d, ³*J*_{H,H} = 9.4 Hz, 1H; H-8), 7.35 (m, 5H; H-7, H-5, H-3, 2H *o*-Ph) 7.20 (m, 3H; 1H *p*-Ph, 2H *m*-Ph), 7.02 (m, 2H; *o*-Ph'), 6.98 (m, 1H; *p*-Ph'), 6.71 (d, 2H; *m*-Ph'), 6.24 (br, 1H; H-11), 5.85 (m, 1H; H-20), 5.02 (m, 2H; H-21), 3.90 (s, 3H; OCH₃), 3.40 (br, 1H; H-12), 3.08 (br, 1H; H-18'), 2.99 (br, 1H; H-14'), 2.60 (m, 2H; H-18, H-14), 2.27 (br, 1H; H-15), 1.90 (br, 1H; H-17), 1.86 (br, 1H; H-16), 1.70 (br, 1H; H-19'), 1.65 (br, 1H; H-17'), 1.52 (br, 1H; H-19). ¹³C NMR (151 MHz, CDCl₃, 25°C): δ (ppm) 158.0 (C-16), 150.5 (d, ²*J*_{C,P} = 7.0 Hz; C-28), 149.9 (d, ²*J*_{C,P} = 6.6 Hz; C-35), 147.3 (C-11), 144.9 (C-13), 142.4 (C-19), 141.8 (C-22), 131.8 (C-18), 129.8 (2C; C-29, C-33), 129.3 (2C; C-36, C-40), 126.8 (C-14), 125.5 (C-31), 125.2 (C-38), 121.9 (C-17), 120.4 (C-12), 120.1 (2C; C-30, C-32), 119.6 (2C; C-37, C-39), 114.5 (C-23), 100.6 (C-15), 60.1 (C-8), 56.5 (C-2), 55.6 (C-21), 42.2 (C-6), 39.7 (C-3), 27.6 (C-5), 27.4 (C-4), 24.7 (C-7). ³¹P NMR (243 MHz, CDCl₃, 25°C): δ (ppm) –11.78.

9-*O*-Diethylphosphorylquinine (**2b**)⁴¹

White solid, yield 56%, m.p. 108–110°C. HRMS (TOF MS ESI): *m/z* calcd for C₂₄H₃₄N₂O₅P⁺: 461.2206 [*M*+H]⁺; found: 461.2202. ¹H NMR

(600 MHz, CDCl_3 , 25°C): δ (ppm) 8.79 (d, $^3J_{\text{H,H}} = 4.4$ Hz, 1H; H-2), 8.05 (d, $^3J_{\text{H,H}} = 9.2$ Hz, 1H; H-8), 7.46 (br, 2H; H-3, H-5), 7.40 (dd, $^4J_{\text{H,H}} = 2.6$ Hz, $^3J_{\text{H,H}} = 9.2$ Hz, 1H; H-7), 5.99 (br, 1H; H-11), 5.87 (m, 1H; H-20), 5.03 (m, 2H; H-21), 4.10 (m, $^3J_{\text{H,H}} = 7.1$ Hz, 1H; H-23a), 3.96 (m, 4H; OCH_3 , H-23b), 3.71 (br, 2H; H-23'), 3.38 (br, 1H; H-12), 3.18 (br, 1H; H-18'), 3.02 (br, 1H; H-14'), 2.64 (br, 1H; H-18), 2.60 (br, 1H; H-14), 2.29 (br, 1H; H-15), 2.00 (br, 1H; H-17), 1.91 (br, 1H; H-16), 1.76 (br, 2H; H-19', H-17'), 1.56 (br, 1H; H-19), 1.23 (t, $^3J_{\text{H,H}} = 7.0$ Hz, 3H; H-24), 0.93 (br, 3H; H-24'). ^{13}C NMR (151 MHz, CDCl_3 , 25°C): δ (ppm) 157.9 (C-16), 147.4 (C-11), 144.8 (C-13), 143.6 (C-19), 141.8 (C-22), 131.8 (C-18), 126.8 (C-14), 121.9 (C-17), 118.6 (C-12), 114.5 (C-23), 101.2 (C-15), 63.9 ($^2J_{\text{C,P}} = 6.0$ Hz; C-28), 63.8 ($^2J_{\text{C,P}} = 6.0$ Hz; C-31), 60.3 (C-8), 56.5 (C-2), 55.7 (C-21), 42.3 (C-6), 39.8 (C-3), 27.7 (C-5), 27.5 (C-4), 24.6 (C-7), 16.0 ($^2J_{\text{C,P}} = 7.6$ Hz; C-29), 15.7 ($^2J_{\text{C,P}} = 7.6$ Hz; C-32). ^{31}P NMR (243 MHz, CDCl_3 , 25°C): δ (ppm) -1.32.

9-*O*-Diphenylphosphorylquinine Hydrochloride ($2a \times \text{HCl}$)

Pale yellow solid, m.p. 112–113°C. ^1H NMR (600 MHz, CDCl_3 , 25°C): δ (ppm) 13.77 (br, 1H; NH^+), 8.67 (s, 1H; H-2), 8.59 (d, $^3J_{\text{H,H}} = 9.0$ Hz, 1H; H-8), 8.26 (s, 1H; H-5), 7.84 (d, $^3J_{\text{H,P}} = 6.6$ Hz, 1H; H-11), 7.78 (s, 1H; H-3), 7.64 (dd, $^4J_{\text{H,H}} = 1.1$ Hz, $^3J_{\text{H,H}} = 9.0$ Hz, 1H; H-7), 7.32 (m, 4H; 2H *o*-Ph, 2H *m*-Ph), 7.26 (m, 2H; *o*-Ph), 7.22 (t, 1H; *p*-Ph), 7.15 (m, 3H; 1H *p*-Ph, 2H *m*-Ph), 5.73 (m, 1H; H-20), 5.12 (m, 2H; H-21), 4.28 (s, 3H; OCH_3), 4.01 (br, 1H; H-18'), 3.58 (br, 1H; H-12), 3.56 (m, 1H; H-14'), 3.25 (m, 2H; H-18, H-14), 2.80 (br, 1H; H-15), 2.25 (br, 2H; H-16, H-17'), 2.09 (br, 1H; H-19'), 1.98 (br, 1H; H-19), 1.92 (br, 1H; H-17'). ^{13}C NMR (151 MHz, CDCl_3 , 25°C): δ (ppm) 162.2 (C-16), 149.9 (d, $^2J_{\text{C,P}} = 7.6$ Hz; C-28), 149.9 (d, $^2J_{\text{C,P}} = 6.0$ Hz; C-35), 149.2 (C-13), 138.2 (C-11), 136.7 (C-22), 134.5 (C-19), 130.2 (2C; C-29, C-33), 130.1 (2C; C-36, C-40), 129.2 (C-14), 127.8 (C-17), 126.2 (C-31), 126.1 (C-38), 123.9 (C-18), 120.0 (C-30), 119.9 (C-32), 119.6 (C-37), 119.6 (C-39), 119.3 (C-12), 118.05 (C-23), 102.2 (C-15), 73.3 (C-9), 59.1 (C-8), 59.0 (C-21), 54.9 (C-2), 43.0 (C-6), 36.8 (C-3), 26.7 (C-4), 24.2 (C-5), 19.1 (C-7). ^{31}P NMR (243 MHz, CDCl_3 , 25°C): δ (ppm) -14.27.

9-*O*-Diethylphosphorylquinine Hydrochloride ($2b \times \text{HCl}$)

Pale yellow solid, m.p. 160–161°C. ^1H NMR (600 MHz, CDCl_3 , 25°C): δ (ppm) 13.74 (br, 1H; NH^+), 8.80 (d, $^3J_{\text{H,H}} = 4.8$ Hz, 1H; H-2), 8.06 (d, $^3J_{\text{H,H}} = 9.6$ Hz, 1H; H-8), 7.81 (br, 1H; H-5), 7.58 (d, $^3J_{\text{H,H}} = 4.2$ Hz, 1H; H-3), 7.46 (dd, $^4J_{\text{H,H}} = 2.4$ Hz, $^3J_{\text{H,H}} = 9.6$ Hz, 1H; H-7), 7.18 (d, $^3J_{\text{H,H}} = 6$ Hz, 1H; H-11), 5.63 (m, 1H; H-20), 5.10 (m, 2H; H-21), 4.29 (m, $^3J_{\text{H,H}} = 7.9$ Hz, 2H; H-23), 4.22 (s, 3H; OCH_3), 4.16 (br, 1H; H-18'), 4.04 (m, $^3J_{\text{H,H}} = 7.2$ Hz, 1H; H-23'a), 3.82 (m, $^3J_{\text{H,H}} = 7.8$ Hz, 1H; H-23'b), 3.50 (t, 1H; H-14'), 3.43 (br, 1H; H-12), 3.19 (br, 1H; H-18), 3.17 (br, 1H; H-14), 2.77 (br, 1H; H-15), 2.25 (br, 2H; H-17', H-19'), 2.19 (br, 1H; H-16), 1.96 (br, 1H; H-19), 1.66 (t, 1H; H-17), 1.43 (t, $^3J_{\text{H,H}} = 7.2$ Hz, 3H; H-24), 1.02 (t, $^3J_{\text{H,H}} = 7.2$ Hz, 3H; H-24'). ^{13}C NMR (151 MHz, CDCl_3 , 25°C): δ (ppm) 159.7 (C-16), 146.6 (C-11), 144.7 (C-13), 140.1 (C-19), 136.9 (C-22), 131.8 (C-18), 125.6 (C-14), 123.8 (C-17), 118.5 (C-12), 117.7 (C-23), 100.8 (C-15), 72.8 (C-9), 65.2 ($^2J_{\text{C,P}} = 5.6$ Hz; C-28), 65.1 ($^2J_{\text{C,P}} = 5.6$ Hz; C-31), 59.4 (C-8), 58.2 (C-21), 54.9 (C-2), 42.9 (C-6), 36.9 (C-3), 26.9 (C-4), 24.2 (C-5), 18.8 (C-7), 16.3 ($^2J_{\text{C,P}} = 6.3$ Hz; C-29), 15.8 ($^2J_{\text{C,P}} = 6.6$ Hz; C-32). ^{31}P NMR (243 MHz, CDCl_3 , 25°C): δ (ppm) -3.27.

RESULTS AND DISCUSSION

Design and Synthesis

Although native and modified quinines have been widely studied for stereoselective applications, the organophosphorus derivatives remain unexplored in this respect. In this work, we envisaged substitution of the hydroxyl group in quinine with a phosphate diester moiety to construct novel chiral receptors for *N*-substituted amino acids. The spatial arrangement of three molecular fragments, the tertiary bicyclic amine (quinuclidine), heteroaromatic system (quinoline) and additional phosphate triester group, provided the possible formation of a cavity that could specifically interact with a variety of ligands. Three types of interactions could be

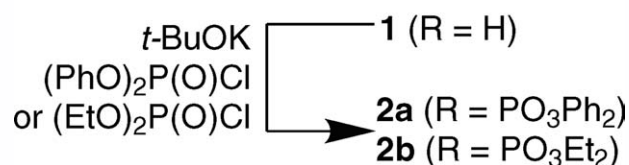
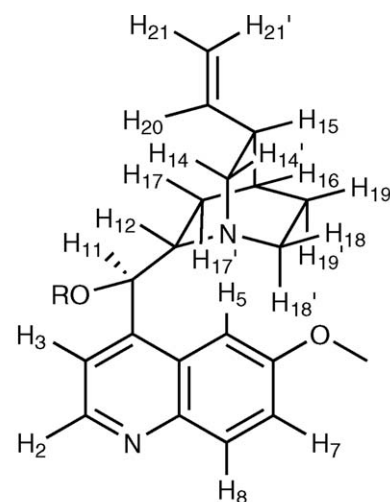


Fig. 1. Synthesis and proton numbering of phosphorylated quinines **2**.

involved in host-guest binding: charge assisted hydrogen bonding between the carboxylic group of the amino acid and the receptor tertiary amine, hydrogen bonding between the amide hydrogen and one of the oxygen atoms of the phosphate and lipophilic or π - π stacking interactions. Importantly, the designed molecules were readily available on a multi-gram scale through a one step synthesis starting from quinine (Fig. 1). Phosphorylation of this substrate with either diphenyl- or diethylchlorophosphate in the presence of potassium *tert*-butoxide allowed us to obtain products **2a** and **2b** in satisfactory yields (66% and 56%, respectively).

Enantiodiscrimination in ^1H NMR

The chiral discriminating potency of novel receptors **2** was tested with the use of a set of ligands possessing different functional groups, namely amino acids, carboxylic acids, amines and alcohols (compounds **3**, Fig. 2). In most cases, both free and protected forms of these analytes were studied. 3,5-Dinitrobenzoyl (DNB) derivatives were used, as the presence of this protecting group enhanced interactions with the electron rich quinoline fragment of the receptor.²⁴ Moreover, the resonances of the protons of the 3,5-dinitrophenyl ring were low-frequency-shifted in the ^1H NMR spectrum, which made them a simple and indicative tool for enantiomeric composition analysis.

CSAs can undergo fast, intermediate or slow exchange with their ligands. In the first case, the NMR spectrum is a weighted average of the bound and unbound ligand and presents two sets of signals derived from the *R* and *S* enantiomers. If enantiomeric discrimination occurs under slow exchange conditions, three signal sets are observed: one for the unbound guest compound and two for each enantiomer bound with the receptor.⁴² According to the theory, fast exchange stereoselective recognition of enantiomers by CSAs occurs when the transient diastereomeric complexes

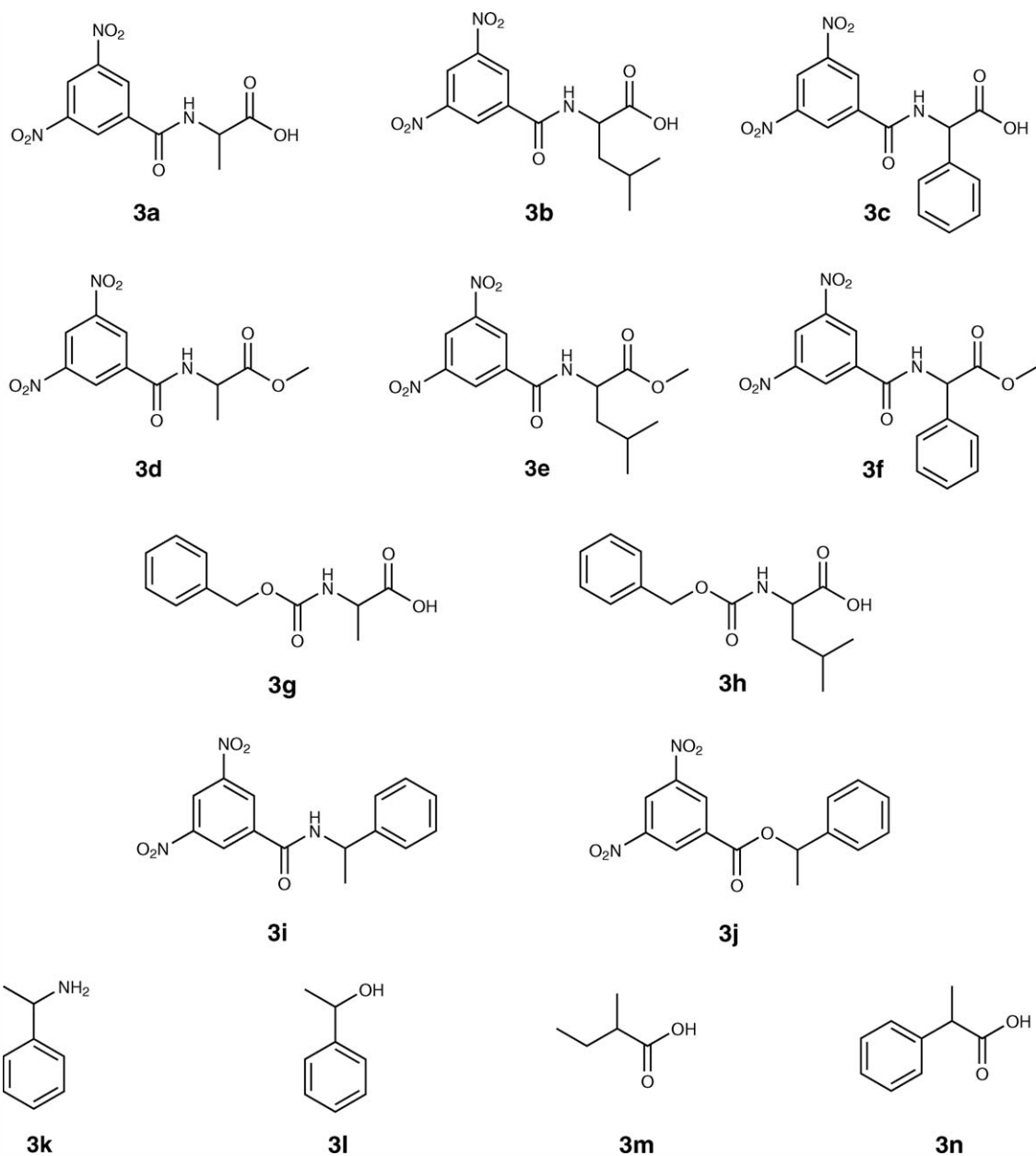


Fig. 2. Structures of the studied ligands.

are characterized by different stereochemical arrangements and/or different association constants. Thus, the concentration of both the selector and selectand); as well as the temperature of the solution may significantly influence the enantiodiscrimination efficiency. The latter factor causes alteration in the association constants and degree of conformational homogeneity of complexes.⁴² In this context, a 50 mM concentration (1:1 molar ratio, Supporting Information Table S1) and a temperature of 283 K (Supporting Information Fig. S1) were chosen as optimal for routine analysis (E).

The studied ligands could be formally divided into four subclasses with respect to the ligand-receptor interactions influencing the enantiodifferentiation efficiency. The first one, *N*-DNB amino acids (compounds **3a-c**), exhibited the highest values of $\Delta\delta$ among all of the explored compounds (a range of 0.1187–0.2320 ppm for the amide protons and

0.0873–0.1979 ppm for the DNB *para* proton). Effective complexation of the DNB-protected amino acids might be associated with three possible intermolecular interactions: a) charge-assisted hydrogen bonding between the carboxylic moiety of the ligand and protonated amine group of the receptor quinuclidine fragment; b) hydrogen bonding between the amide NH of the DNB amino acid and OH of **1** or oxygen atom of the phosphate moiety of **2**; and c) π -stacking interactions between the electron poor DNB group and electron rich quinoline ring of the receptor molecule. Within the second subclass of ligands, DNB amino acid methyl esters (compounds **3d-f**), medium enantiodiscrimination efficiency was observed ($\Delta\delta$ in the range of 0.0122–0.0526 ppm for the NH proton and 0.0031–0.0194 ppm for the DNB *para* proton). The structure of **3d-f** offers only two possible interactions with the host molecule, namely hydrogen bonding and π -stacking what explains the diminished values of chemi-

TABLE 1. Enantiodifferentiation efficiency of native (1**) and phosphorylated quinines (**2**), expressed as the chemical shift nonequivalences ($\Delta\delta$) observed by ^1H NMR for racemic mixtures of ligands **3** in the presence of the hosts measured under optimized conditions (50:50 mM ratio, 283 K)**

Ligand	Proton	$\Delta\delta$ (ppm)			
		1	2a	2b	2b \times HCl
3a	<i>o</i> -H	0.037	0.023	0.115 ^a	0.034
	<i>p</i> -H	0.031 ^a	0.035	0.189 ^a	0.031
	NH	0.124	0.232	0.101	0.037
	CH _{α}	0.036	0.020	0.155	0.029
	CH ₃	0.016	0.023	0.030	–
3b	<i>o</i> -H	0.006	0.042	0.107	0.025
	<i>p</i> -H	0.028	0.073	0.198	0.022
	NH	0.106	0.119	0.094	–
	CH _{α}	0.073	0.044 ^a	0.121	–
	CH ₃	0.029	0.010	0.003	–
3c	CH ₃	0.027	0.004	0.007	–
	<i>o</i> -H	0.014 ^a	–	0.075	0.010
	<i>p</i> -H	0.012 ^a	0.031	0.087	0.008
	NH	0.081	0.168	~ 0.119	–
	CH _{α}	–	0.079	0.038	0.005
3d	<i>o</i> -H	–	–	–	0.014
	<i>p</i> -H	–	–	0.004	0.016
	NH	–	0.036	0.053	–
	CH _{α}	–	0.002	0.006	0.002
	OMe	0.002	0.003	0.002	0.004
3e	CH ₃	–	0.013	0.012	0.003
	<i>o</i> -H	–	0.003	0.004	0.014
	<i>p</i> -H	–	0.003	0.016	0.019
	NH	0.007	0.032	0.038	0.021
	OMe	0.002	0.003	0.003	0.002
3f	CH ₃	–	0.006	^a	^a
	CH ₃	–	0.015	^a	^a
	<i>p</i> -H	–	–	–	0.003
	CH _{α}	0.003	–	0.004	0.005
	NH	–	–	0.012	0.003
3g	CH _{α}	–	0.040	0.044	–
	NH	0.079	–	0.044	^a
	CH ₃	0.018	–	^a	^a
3h	CH _{α}	0.040	0.042 ^a	0.036	–
	CH ₃	0.006	0.018	0.006	–
	CH ₃	0.020	0.016	0.003	–
3i	<i>o</i> -H	–	–	0.002	0.004
	<i>p</i> -H	0.003	–	0.006	0.004
	CH ₃	–	–	–	0.002
3j	CH ₃	–	–	–	0.001
3k	–	–	–	–	–
3l	CH ₃	0.007	0.003	0.002	–
3m	CHCH ₃	0.032	0.004	0.006	0.002
	CH ₂ CH ₃	0.013	0.001	–	–
3n	CH _{α}	0.033	0.010 ^a	0.003	0.005

^aOverlapping signals.

cal shift nonequivalence in comparison to the free acids. The loss in enantioselective efficiency of *N*-benzyloxycarbonyl protected amino acids (compounds **3g** and **3h**) probably resulted from weaker lipophilic interactions of the receptor with the phenyl ring of the Cbz-protecting group than with the significantly electron-poorer DNB fragment. The remaining compounds (**3i–3n**) exhibited the lowest enantiodiscrimination which was likely the result of a limited number of potential contacts.

The results presented in Table 1 allowed a comprehensive comparison between the modified and nonmodified quinines

with respect to their enantiodiscrimination efficiency. In general, the phosphorylated hosts appeared to be privileged with respect to native quinine, and this was general across all three groups of amino acid derivatives (**3a–h**). Interestingly, different patterns of ^1H resonance differentiation upon complexation with **2a** and **2b** were observed for the *N*-DNB free acids (**3a–c**). The diphenyl phosphate derivative (**2a**) showed the greatest influence on the $\Delta\delta$ of the ligand amide proton, whereas the diethyl phosphate derivative (**2b**) had the greatest influence on the $\Delta\delta$ of the aromatic protons of the *N*-protecting group. As expected, the hydrochloride salt **2b** \times HCl lost the efficiency of the corresponding nonprotonated amine because of an alteration of the host-guest ion pair formation. For practical applications, **2b** is recommended, as it differentiated enantiomers the most clearly through low-frequency-shifted resonances in a noncrowded region of the ^1H spectrum (as exemplified in Fig. 3).

For the group of methyl esters (**3d–f**), the discrimination properties of all quinine derivatives was significantly decreased, particularly in the case of the native one, due to the loss of ion pairing. The highest values of $\Delta\delta$ were observed for the amide guest proton upon complexation with **2b**. It is worth noting that the same receptor in the form of its hydrochloride salt (**2b** \times HCl) was quite effective, inducing particularly high $\Delta\delta$ values for the DNB aromatic protons (poorly separated by the other selectors). These observations could be explained by a difference in the number of potential hydrogen bonds formed in the complex. For the nonprotonated forms, only one such specific contact can be formed, whereas in the case of **2b** \times HCl, there is the possibility of additional bonding where the quaternary ammonium group can serve as the donor. *N*-Cbz substitution of the amino acids resulted in a group of compounds that produced moderate chemical shift nonequivalences with hosts **1**, **2a** and **2b**, and a lack of enantiodiscrimination for the hydrochloride of **2b**. For the final set of monofunctionalized compounds (**3i–n**), the studied effect was less significant and irregularly depended on the kind and state (protected or not) of the heteroatom moiety present in their structure. Thus, the DNB protected amine **3i** and alcohol **3j** enantiomers were the most efficiently distinguished by **2b** \times HCl, with efficiency similar to the DNB amino acid methyl esters. On the

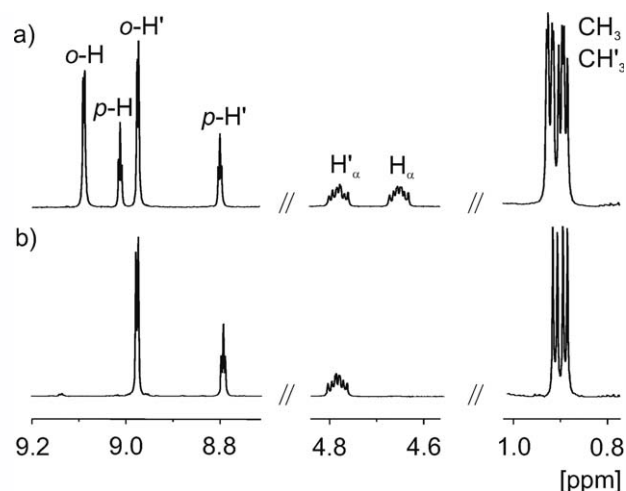


Fig. 3. Selected resonances of the racemic mixture (a) and *S* enantiomer (b) of **3b** in ^1H NMR spectra in the presence of **2b** (50:50 mM ratio, 283 K).

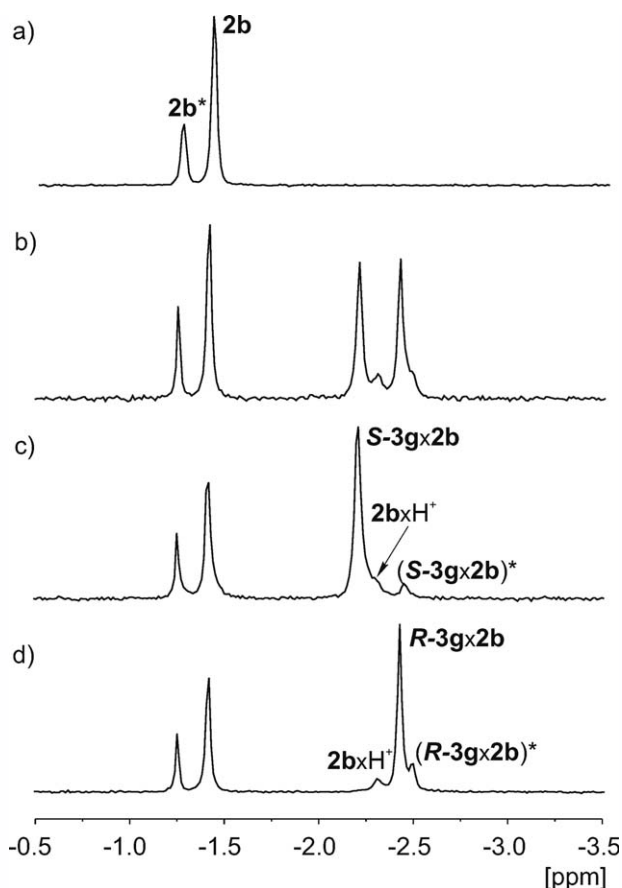


Fig. 4. Frozen conformational equilibrium of **2b** and the enantiodifferentiation effect under slow exchange conditions illustrated by the ^{31}P NMR spectra of the free selector (a) and its complexes with racemic (b) and enantiomerically pure (c and d) Cbz-Ala ligand (**3g**) (10:5 mM ratio, 180 K).

other hand, nonfunctionalized quinine was the compound of choice for carboxylic acids (**3m** and **3n**), which is in agreement with the literature data.²⁵ This CSA also gave the highest $\Delta\delta$ value for racemic phenylethanol (**3l**). In summary, except for the last three mentioned cases, the novel phosphorus quinines appear to be superior CSAs compared to the nonmodified ones.

Enantiodiscrimination in ^{31}P NMR

Using the presence of a phosphorus atom as the characteristic feature of the novel compounds, the enantiodifferentiation phenomenon could also be studied by means of ^{31}P NMR. Phosphorus resonance spectra are much more straightforward for interpretation in comparison to proton spectra. However, no discrimination effect was observed in preliminary experiments at room temperature because of fast exchange between host molecules unbound and bound with the ligands. To achieve slow exchange conditions and to elucidate the ^{31}P NMR resonances derived from the *R* and *S* enantiomers complexed with the CSA, the temperature of the experiments was decreased to 180 K. The spectrum of phosphorylated receptor **2b** acquired under such conditions revealed resonances of particular conformations, with two predominating (Fig. 4a).

Subsequently, the conditions of the low temperature experiments were optimized using the selected ligand (**3h**) by changing its concentration at a constant host (**2b**) con-

centration (10 mM). At this concentration, no precipitation of the substrate or complex occurred. The ligand concentration was finally adjusted at 5.0 mM at a host-guest ratio of 1:2, which ensured complete ligand binding and thus reliable enantiomer composition analysis.

Four different patterns in the ^{31}P NMR spectra were observed (Table 2). The most preferred case for analysis was found for *N*-substituted amino acids (**3a**, **3b**, **3g** and **3h**) and 2-phenylpropionic acid (**3n**). Here, proton transfer between the carboxylic acid and amine must have occurred, and the ion pairing and other interactions were apparently strong enough to reach slow exchange conditions on the NMR time scale at the applied temperature of 180 K. As a result, the ^{31}P NMR spectra revealed signals derived from two nonbound excess **2b** conformers (−1.26 ppm, −1.42 ppm), a novel one originating from its protonated form (−2.31 ppm) and those resulting from **2b** complexed with the ligand enantiomers. For complexes of **2b** with *N*-benzyloxycarbonylamino acids **3g** and **3h**, each enantiomer showed two ^{31}P resonances (one significantly predominated, Figs. 4b–4d and Table 2), while the complexes of enantiomers of the DNB derivatives **3a** and **3b** showed one or two signals. Phenylpropionic acid (**3n**) represented the simplest instance, as each stereoisomer formed a complex producing one signal.

In the case of compound **3m**, apart from the free and protonated **2b** signals, just one novel resonance was registered, and it did not depend on the enantiomeric composition. The observed peak broadening could suggest that the spectra were recorded under medium exchange conditions. This would result from the ligand-receptor interactions being too weak to achieve slow exchange under the experimental conditions (180 K).

For the complexation of **2b** with DNB-amino esters (**3d–f**), 1-phenylethylamine (**3i**) and nonprotected 1-phenylethanol (**3l**), a high frequency shift of both conformer resonances was detected that represented a weighted average of bound and unbound quinine. For the remaining compounds (**3j** and

TABLE 2. ^{31}P NMR chemical shifts (δ) observed for **2b** in the presence of racemic mixtures of the analyzed ligands **3** at 180 K (10:5 mM ratio) and the percentage of each conformer in parentheses. Entries indicating medium or fast exchange conditions between complexed and free quinine **2b** are marked in *italics*

Ligand	δ (ppm)	
	2b × <i>S</i> -ligand	2b × <i>R</i> -ligand
3a	−1.08	−2.41 (84%); −2.59 (16%)
3b	−0.84 (59%); −2.41 (41%)	−2.50
3d	−1.53 (25%); −2.44 (75%)	
3e	−1.53 (26%); −2.57 (74%)	
3f	−1.53 (25%); −2.44 (75%)	
3g	−2.21 (91%); −2.46 (9%)	−2.43 (85%); −2.50 (15%)
3h	−2.16 (93%); −2.49 (7%)	−2.50 ^a
3i	−1.77 (26%); −2.32 (74%)	
3j	No interaction	
3k	No interaction	
3l	−1.29 (24%); −1.49 (76%)	
3m	−2.14	
3n	−2.14	−2.22

^aTwo signals overlapping.

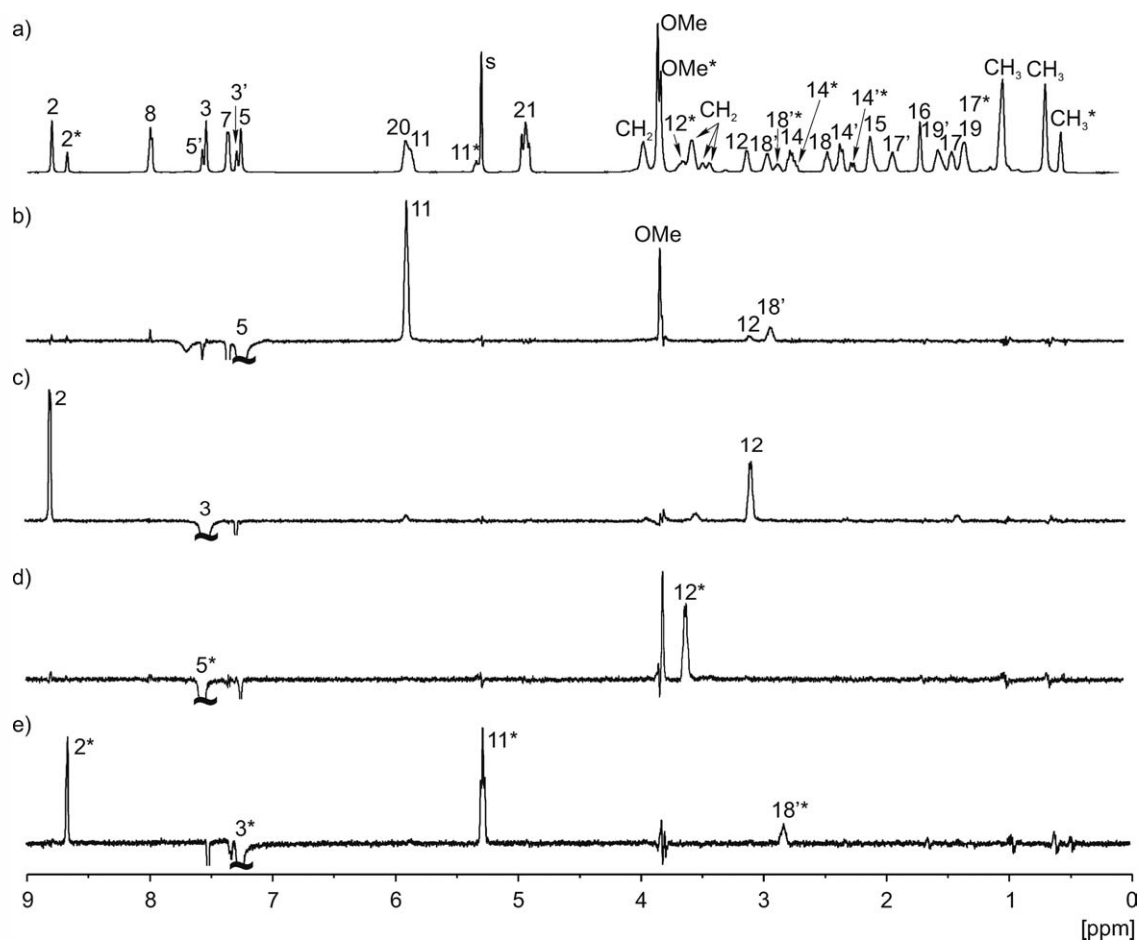


Fig. 5. ^1H NMR (a) and 1D ROESY (b–e) spectra of **2b** at 200 K, with the protons important for conformational analysis (H3 and H5 of both conformers) irradiated. * – signals derived from the less populated conformation.

3k), no specific host-guest complex resonances were observed.

Conformational Analysis of Phosphorylated Quinines

The conformation of the chiral selector is of a great importance to its enantiodiscriminating properties, as it determines the functionality and size of the binding site. Therefore, the conformations of CSAs **2**, in their free and protonated forms (the later resembling a state formed upon complexation of an acid), were studied by means of selective 1D and 2D ROESY experiments. The stereochemistry of quinine and its derivatives can be described in term of rotations around the C8–C9 and C9–C13 bonds. It has previously been established that cinchona alkaloids can, in principle, adopt four different conformations, two open and two closed (Supporting Information Fig. S2).^{26,43} In the open states, the quinuclidine nitrogen atom is situated remotely from the quinoline ring, while in the closed conformers, it points toward the quinoline ring. Thus, intramolecular ROEs between the quinoline H17 and H18 protons and quinuclidine H3 and H5 protons, along with ROEs involving H11 and H12, are the most diagnostic tools for identification of the rotamers. The different conformational states involve changes in the H11–C9–C8–H12 dihedral angle, which is reflected in the values of the $^3J_{\text{H11,H12}}$ coupling constants measured in the NMR spectra. It has been reported in the literature that parent quinine prefers an open

conformation in solution.^{2,44} In NMR studies on chiral recognition phenomena, this arrangement is considered to be responsible for its enantiodiscrimination abilities, as the unhindered quinuclidine nitrogen is able to form strong interactions with analytes.

Conformational studies of phosphorylated quinine derivatives **2a** and **2b** were difficult to perform at room temperature, as the ^1H NMR spectra showed significant broadening of a majority of the ^1H resonances. This included the signal of proton H11, key for conformational analysis, which was almost flattened. Moreover, the quinuclidine H3 and H5 resonances overlapped in the spectrum of **2b**. Thus, the temperature of the experiments was decreased to 200 K to achieve slow exchange conditions and allow for reliable analysis of the existing conformational arrangement. The ^1H NMR spectrum of **2b** revealed two frozen rotational states present in a 73:27 ratio (Fig. 5a). This observation was well correlated with the ^{31}P NMR spectrum, which showed two resonances (73:27 molar ratio) at -1.42 ppm and -1.26 ppm, respectively.

ROEs H5–H11, H5–H18 and H3–H12, characteristic of closed conformation **2**, were detected for the more populated species in the 1D ROESY spectra (Fig. 5). In the case of the minor rotamer, the presence of intense H3*–H11*, H3*–H18* and H5*–H12* contacts indicated the closed conformation **1**. Unfortunately, the vicinal coupling $^3J_{\text{H11,H12}}$ values were not

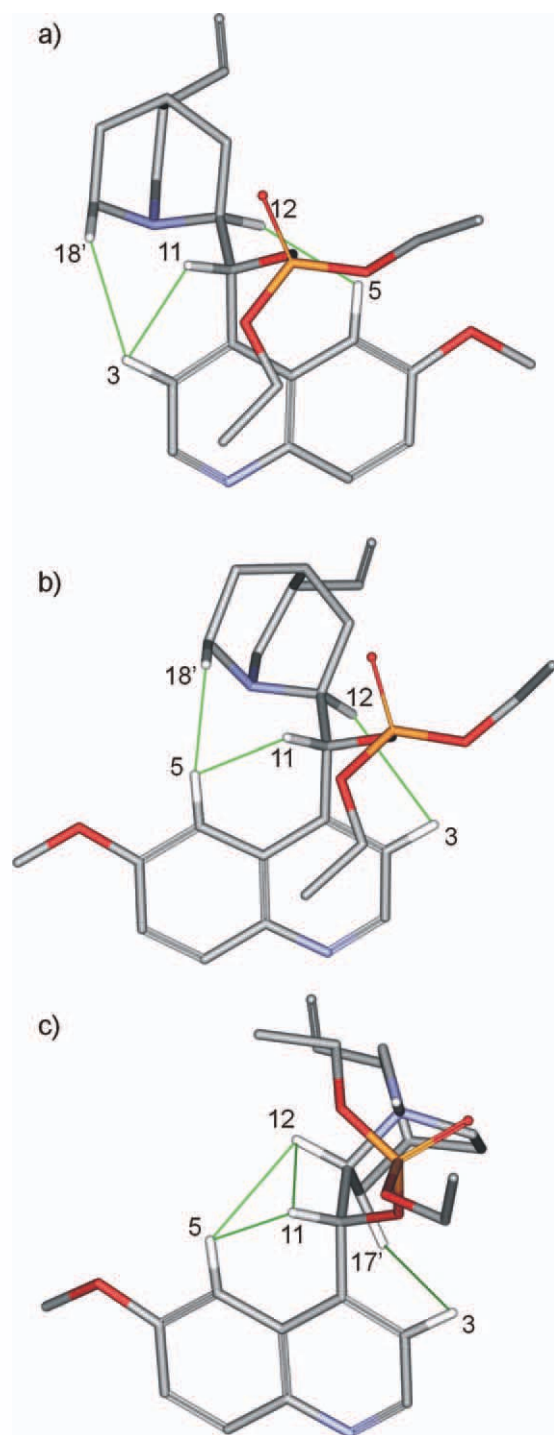


Fig. 6. Conformations of phosphorylated quinine derivative **2b** (minor – closed 1 and major – closed 2, panels a and b, respectively) and its hydrochloride **2b**×HCl (open 3, panel c) modeled based on the 1D ROESY experiments. Indicative interproton contacts are marked as solid green lines. [Color figure can be viewed in the online issue, which is available at [wileyonlinelibrary.com](http://www.wileyonlinelibrary.com).]

determined because of signal overlap. Using interproton contacts obtained from NMR studies, the structures of both **2b** conformers were modeled (Figs. 6a and 6b).

Analogous to **2b**, the diphenyl ester was present in a 68:32 ratio (^{31}P NMR δ –10.64 ppm and –11.08 ppm, respectively). The measured vicinal coupling constants $^3J_{\text{H11,H12}}$ were equal to 8.5 Hz for the predominating rotamer and 10.3 Hz for the

less populated one; these values are characteristic of closed arrangements. Their existence was also evident by comparison of the H11–H18' and H11–H12 ROEs, for which the former was more intense than the latter (Supporting Information Fig. S3). In the case of the less populated species, the presence of the ROEs H3*–H18'* and H3*–H11* confirmed the existence of closed conformer 1. Because of signal overlap of the quinoline and phenyl protons, interactions characteristic of closed conformation 2, including those originating from the H5 proton, were undetectable. However, the major closed conformer 2 was indicated by the H11 and H5 ROE and vicinal coupling constants $^3J_{\text{H11,H12}} = 8.5$ Hz. The structures of the conformers of **2a** modeled based on the NMR data (Supporting Information Figs. S4a and S4b) were similar to those found for **2b**. In summary, both phosphorylated quinines **2a** and **2b** adopt two closed conformations, with form 2 predominating.

Regarding the diphenyl and diethyl ester moieties, no dipolar interactions with the quinoline or quinuclidine protons of **2a** and **2b** were detected in the 1D and 2D ROESY experiments (carried out at 200 K as well as at 298 and 283 K at a spin lock time of 100–1200 ms). This indicated that the organophosphorus fragments are located externally to the alkaloid core.

Protonation of quinine derivatives **2a** and **2b** significantly changes their conformational status. The ROE effects protons H3–H17' and H11–H5 detected for **2b**×HCl clearly indicated the presence of open conformer 3. This was further supported by the stronger interaction of H11 with H12 when compared to H11–H18' (Fig. 7). The corresponding ROEs, indicative of open conformation 3, were also present in **2a**×HCl (Supporting Information Fig. S5). Finally, the presence of the open conformation of both protonated quinines was supported by loss of the $^3J_{\text{H11,H12}}$ in comparison with the values of the corresponding coupling constant in their free forms.

The presence of an intramolecular hydrogen bond between the NH and phosphate moiety, which stabilizes open conformation 3, was confirmed in the modeled structures of both protonated **2a** and **2b** (Supporting Information Figs. S4c and S6c, respectively).

The architecture, to some extent complementary to the NMR data, was established for the solid state structure of **2b**×HCl dichloromethane hemisolvate, which was determined by single-crystal X-ray diffraction analysis (Fig. 8 and Supporting Information Table S2). The adopted open conformation 3 of **2bH**⁺ (similar to that of quininium cation found in its crystalline derivatives)^{45–48} showed intramolecular distances of H3–H17' and H5–H11 equal to 2.25 and 2.09 Å, respectively. The arrangement of the three structural parts (quinoline, quinuclidine and phosphate ester) formed a cavity where a chlorine ion and partially a molecule of solvent (dichloromethane) were located. However, in this case, the positively charged amine group formed the ion pair with chlorine (Fig. 8 and Supporting Information Table S3), in contrast to the NH–phosphate contact modeled in solution.

Conformational Analysis of Complexes of *N*-Cbz-Leucine (**3h**) with **2b**

Because the conformational changes of chiral selectors upon analyte binding are crucial for understanding of the chiral recognition process, selected diastereomeric complexes (**3h**×**2b**) were investigated in detail. For **R-3h**×**2b**, the

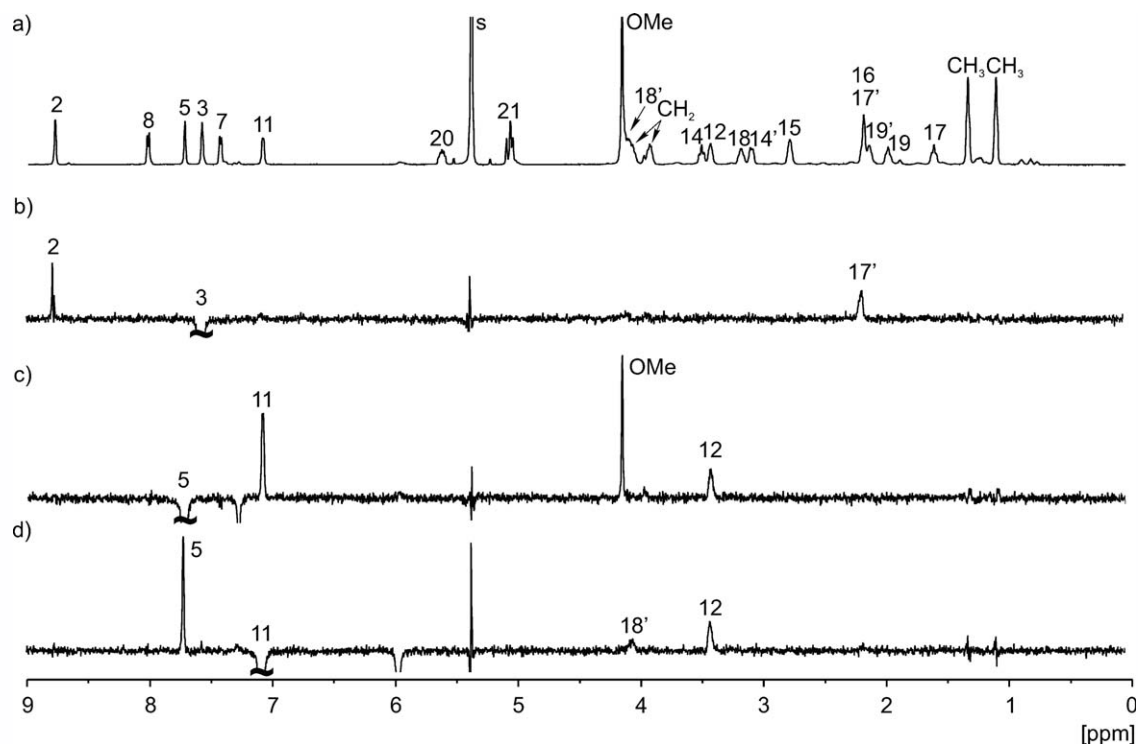


Fig. 7. ^1H NMR (a) and 1D ROESY (b-d) spectra of $2\mathbf{b}\times\text{HCl}$ at 200 K, with the protons important for conformational analysis (H3, H5 and H11) irradiated.

presence of ROEs H3-H17' and H5-H11, along with H11-H12 being more pronounced than H11-H18', indicated open conformation 3 (Supporting Information Fig. S6). The situation was less clear for the opposite enantiomer because the H3

and H5 protons were superimposed (Supporting Information Fig. S7). Nevertheless, the ROE involving proton H17' suggested the presence of the open 3 or open 4 form. The modeling studies (see below) favored the former option. Thus, $2\mathbf{b}$ interacts with each enantiomer of $3\mathbf{h}$, changing its native conformation into open 3, which corresponds well with that adopted by the protonated form $2\mathbf{b}\times\text{HCl}$.

Because the ROESY experiments did not show intermolecular contacts, complexation-induced shifts of selector $2\mathbf{b}$ protons upon the binding of either $R\text{-}3\mathbf{h}$ or $S\text{-}3\mathbf{h}$ were assessed to gain insight into the interactions. To exclude the chemical shift changes resulting from conformational changes upon protonation, the values measured for $2\mathbf{b}\times\text{HCl}$ were subtracted from those registered for $3\mathbf{h}\times 2\mathbf{b}$ (Fig. 9).

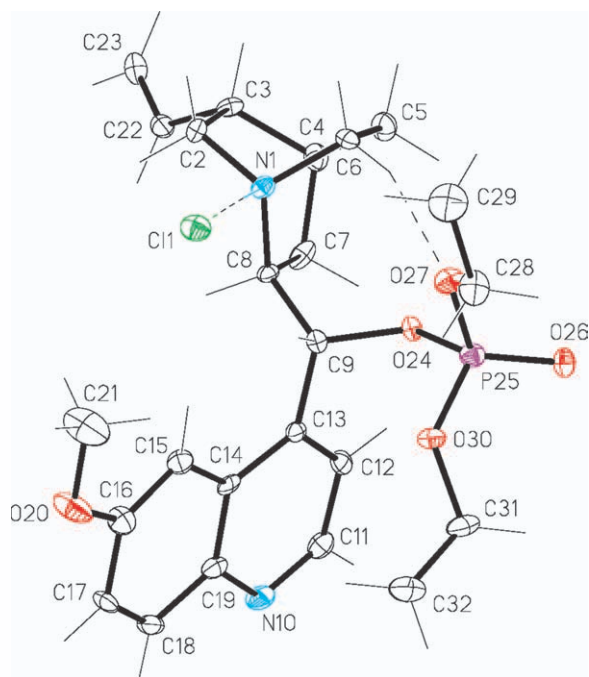


Fig. 8. Molecular structure of $2\mathbf{b}\times\text{HCl}\times 0.5\text{CH}_2\text{Cl}_2$ (with the atom-numbering scheme) joined via charge-assisted N-H...Cl hydrogen bond (H...Cl 2.09 Å, N...Cl 3.022(3) Å, N-H...Cl 177°; dashed line) with Cl^- in the crystal of $(\text{C}_{24}\text{H}_{34}\text{N}_2\text{O}_5\text{P}^+)\text{Cl}^-\times 0.5\text{CH}_2\text{Cl}_2$. Intramolecular C-H...O contact (H...O 2.46 Å, C...O 3.406(4) Å, C-H...O 161°) is also shown. Displacement ellipsoids represent the 40% probability level. [Color figure can be viewed in the online issue, which is available at [wileyonlinelibrary.com](http://www.wileyonlinelibrary.com).]

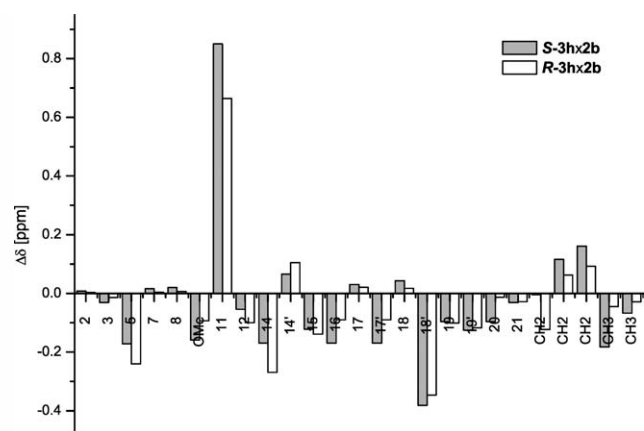


Fig. 9. Differences between the chemical shifts of the complexed quinine receptor and its protonated form: $S\text{-}3\mathbf{h}\times 2\mathbf{b} - 2\mathbf{b}\times\text{HCl}$ and $R\text{-}3\mathbf{h}\times 2\mathbf{b} - 2\mathbf{b}\times\text{HCl}$.

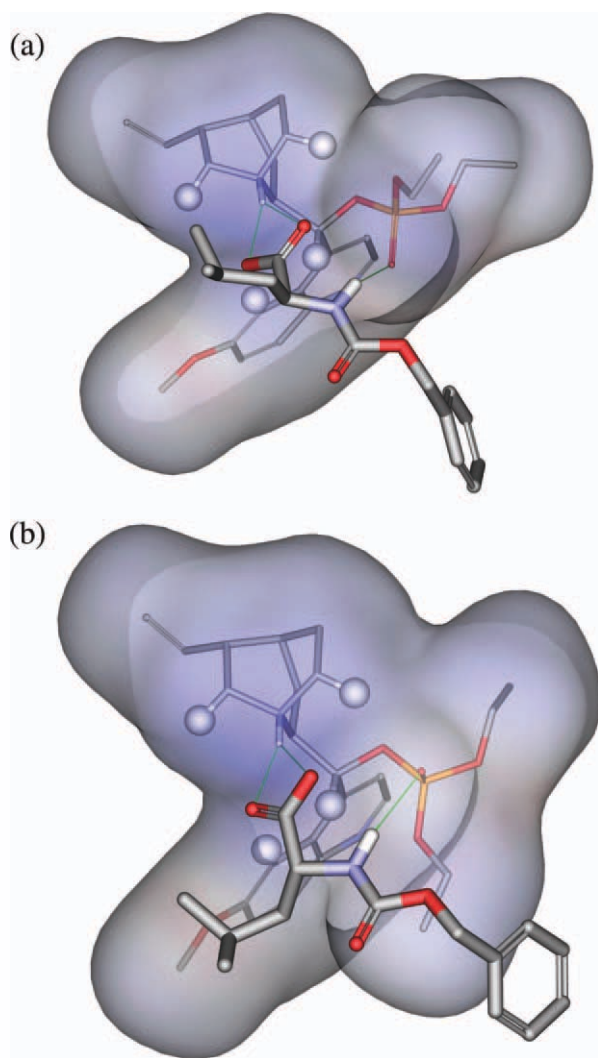


Fig. 10. Models of the *S*-**3h**×**2b** and *R*-**3h**×**2b** complexes (panels a and b, respectively). The molecular surface of the receptor was colored according to interpolated charge. Hydrogen bonds are marked as green solid lines. Protons showing high complexation-induced shifts (H5, H11, H14, H18') are marked as white spheres. [Color figure can be viewed in the online issue, which is available at wileyonlinelibrary.com.]

The overall patterns of complexation-induced shifts were similar to each other for both complexes. The highest absolute values were observed for H11, H14, and H18' if considering the aliphatic part and H5 for the aromatic portion. These protons are located inside the cavity formed by the host molecule in open conformation **3**. Using an NMR data-based model (Fig. 10), a charge assisted hydrogen bond between the ligand carboxylic group and protonated **2b** amine moiety as well as a hydrogen bond between the phosphate oxygen atom of **2b** and the NH of **3h** were found to be crucial stabilizing forces of the complex. Significantly, the phosphate group appeared to be essential for effective complexation and enantiodiscrimination in comparison to the native quinine. When comparing enantiomer binding, it is clear that the H_α proton of the ligands significantly changes in terms of chemical environment. It is pointed toward the cavity for the *S* stereoisomer and exposed to the solvent for the *R* enantiomer. Such a difference can reflect in the high enantiodiscrimination ($\Delta\delta$) observed for this proton (Table 1).

CONCLUSIONS

The structural and functional elements of the quinine molecule are assembled in a unique, characteristic three-dimensional arrangement that makes this compound exceptionally useful in stereoselective applications. Additionally, the presence of reactive groups allows further development/modification of the native compound to adjust its properties. Transformations of the C-9 hydroxyl group to esters or carbamates, described in the literature seem to be the most common synthetic approaches to new compounds in this series. In this respect, we envisaged and validated phosphorylated quinines as effective CSAs. These compounds induced chemical shift nonequivalences of the ¹H and ³¹P NMR signals in a set of racemic analytes. Diethyl and diphenyl phosphate derivatives showed a high degree of complementarity for protected amino acids and outdistanced the native quinine action in this respect, which confirmed our design approach. The proposed protocol based on ¹H NMR can be considered an alternative for the routine analysis of enantiomer composition. The enantiodiscrimination effect was rationalized in terms of molecular interactions between the host and guest molecules. The NMR data and modeling studies defined the polar contacts as the major forces responsible for the ligand affinity for the receptors, with essential participation of the phosphate group. Conformational rearrangement involving a switch from a closed to an open species further illustrated the process of adduct formation.

As the quinine phosphates are readily prepared, other stereoselective applications, such as enantioselective catalysis or chiral separation techniques can be easily foreseen as a continuation of these studies. Furthermore, the phosphorus moiety offers possibilities in terms of subsequent transformations, such as selective and exhaustive hydrolysis and transesterification of the phenyl groups. Such features make the described quinine derivatives promising and versatile chiral discriminators of general relevance.

ACKNOWLEDGMENTS

Calculations were performed using the software resources from the Wrocław Centre for Networking and Supercomputing.

LITERATURE CITED

1. Yoon TP, Jacobsen EN. Privileged chiral catalysts. *Science* 2003;299:1691–1693.
2. Uccello-Barretta G, Balzano F, Quintavalli C, Salvadori P. Different enantioselective interaction pathways induced by derivatized quinines. *J Org Chem* 2000;65:3596–3602.
3. Maier NM, Schefzick S, Lombardo GM, Feliz M, Rissanen K, Lindner W, Lipkowitz KB. Elucidation of the chiral recognition mechanism of *Cinchona* alkaloid carbamate-type receptors for 3,5-dinitrobenzoyl amino acids. *J Am Chem Soc* 2002;124:8611–8629.
4. Czerwenka C, Zhang MM, Kähhlig H, Maier NM, Lipkowitz KB, Lindner W. Chiral recognition of peptide enantiomers by *Cinchona* alkaloid derived chiral selectors: mechanistic investigations by liquid chromatography, NMR spectroscopy, and molecular modeling. *J Org Chem* 2003;68:315–3327.
5. Uccello-Barretta G, Balzano F, Salvadori P. Rationalization of the multireceptorial character of chiral solvating agents based on quinine and its derivatives: overview of selected NMR investigations. *Chirality* 2005;17:S243–S248.
6. Bicker W, Chiorescu I, Arion VB, Lämmerhofer M, Lindner W. Contributions to chromatographic chiral recognition of permethrinic acid stereoisomers by a quinine carbamate chiral selector: evidence from X-ray diffraction, DFT computations, ¹H NMR, and thermodynamic studies. *Tetrahedron: Asymmetry* 2008;19:97–110.

- Uccello-Barretta G, Balzano F, Bardoni S, Vanni L, Giurato L, Guccione S. Chiral discrimination processes by C9 carbamate derivatives of dihydroquinine: interaction mechanisms of diastereoisomeric 9-O-(S)- or (R)-1-(1-Naphthyl)ethylcarbamate]dihydroquinine and the two enantiomers of N-(3,5-Dinitrobenzoyl)alanine methyl ester. *Tetrahedron: Asymmetry* 2008;19:1084–1093.
- Kacprzak K, Gawroński J. *Cinchona* alkaloids and their derivatives: versatile catalysts and ligands in asymmetric synthesis. *Synthesis* 2001;961–998.
- Lämmerhofer M, Hebenstreit D, Gavioli E, Lindner W, Mucha A, Kafarski P, Wieczorek P. High-performance liquid chromatographic enantiomer separation and determination of absolute configurations of phosphinic acid analogues of dipeptides and their alpha-aminophosphinic acid precursors. *Tetrahedron-Asymmetry* 2003;14:2557–2565.
- Lämmerhofer M. Chiral separations by capillary electromigration techniques in nonaqueous media: II. enantioselective nonaqueous capillary electrochromatography. *J Chrom A* 2005;1068:31–57.
- Gübitz G, Schmid MG. Advances in chiral separation using capillary electromigration techniques. *Electrophoresis* 2007;28:114–126.
- Lämmerhofer M. Chiral recognition by enantioselective liquid chromatography: mechanisms and modern chiral stationary phases. *J Chrom A* 2010;1217:814–856.
- Lämmerhofer M. Chiral separations by capillary electromigration techniques in nonaqueous media: I. enantioselective nonaqueous capillary electrophoresis. *J Chrom A* 2005;1068:3–30.
- Rosini C, Uccello-Barretta G, Pini D, Abete C, Salvadori P. Quinine: an inexpensive chiral solvating agent for the determination of enantiomeric composition of binaphthyl derivatives and alkylarylcarbinols by NMR spectroscopy. *J Org Chem* 1988;53:4579–4581.
- Salvadori P, Pini D, Rosini C, Bertucci C, Uccello-Barretta G. Chiral discriminations with *Cinchona* alkaloids. *Chirality* 1992;4:43–49.
- Van Oeveren A, Menge W, Feringa BL. Enantioselective synthesis of furfuralcohols by catalytic asymmetric addition of diethylzinc to furanaldhydes. *Tetrahedron Lett* 1989;30:6427–6430.
- Uccello-Barretta G, Pini D, Mastantuono A, Salvadori P. Direct NMR assay of enantiomeric purity of chiral β -hydroxy esters by using quinine as chiral solvating agent. *Tetrahedron: Asymmetry* 1995;6:1965–1972.
- Klein J, Hartenstein H, Sicker D. First discrimination of enantiomeric cyclic hemiacetals and methyl acetals derived from hydroxamic acids and lactams of Gramineae by means of ^1H NMR using various chiral solvating agents. *Magn Reson Chem* 1994;32:727–731.
- Abid M, Török B. *Cinchona* alkaloid induced chiral discrimination for the determination of enantiomeric composition of alpha-trifluoromethylated-hydroxyl compounds by ^{19}F NMR spectroscopy. *Tetrahedron: Asymmetry* 2005;16:1547–1555.
- Zymanczyk-Duda E, Skwarczynski M, Lejczak B, Kafarski P. Accurate assay of enantiopurity of 1-hydroxy- and 2-hydroxyalkylphosphonates esters. *Tetrahedron: Asymmetry* 1996;7:1277–1280.
- Maly A, Lejczak B, Kafarski P. Quinine as chiral discriminator for determination of enantiomeric excess of diethyl 1,2-dihydroxyalkylphosphonates. *Tetrahedron: Asymmetry* 2003;14:1019–1024.
- Rudzinska E, Berlicki L, Kafarski P, Lämmerhofer M, Mucha A. *Cinchona* alkaloids as privileged chiral solvating agents for enantiodiscrimination of N-protected aminoalkylphosphonates—a comparative NMR study. *Tetrahedron Asymmetry* 2009;20:2709–2714.
- Klein J, Borsdorf R. NMR spectroscopic determination of enantiomers via their triphenyltin derivatives: a new application of chiral solvating agents. *Fresenius J Anal Chem* 1994;350:644–646.
- Uccello-Barretta G, Bardoni S, Balzano F, Salvadori P. Versatile chiral auxiliaries for NMR spectroscopy based on carbamoyl derivatives of dihydroquinine. *Tetrahedron: Asymmetry* 2001;12:2019–2023.
- Uccello-Barretta G, Mirabella F, Balzano F, Salvadori P. C11 versus C9 carbamoylation of quinine: a new class of versatile polyfunctional chiral solvating agents. *Tetrahedron: Asymmetry* 2003;14:1511–1516.
- Uccello-Barretta G, Vanni L, Balzano F. NMR enantiodiscrimination phenomena by quinine C9-carbamates. *Eur J Org Chem* 2009;860–869.
- Uccello-Barretta G, Vanni L, Berni MG, Balzano F. NMR enantiodiscrimination by pentafluorophenylcarbamoyl derivatives of quinine: C10 versus C9 derivatization. *Chirality* 2011;23:417–423.
- Mlynarz P, Rudzinska E, Berlicki L, Kafarski P. Organophosphorus supramolecular chemistry. Part 2. Organophosphorus receptors. *Curr Org Chem* 2007;11:1593–1609.
- Wenzel TJ, Chisholm CD. Using NMR spectroscopic methods to determine enantiomeric purity and assign absolute stereochemistry. *Prog Nucl Magn Reson Spectrosc* 2011;59:1–63.
- Harger MJP. Chemical shift non-equivalence of enantiomers in the proton magnetic resonance spectra of partly resolved phosphinothioic acids. *J Chem Soc Perkin Trans 2* 1978;326–331.
- Omelanczuk J, Mikołajczyk M. Chiral t-butylphenylphosphinothioic acid: a useful chiral solvating agent for direct determination of enantiomeric purity of alcohols, thiols, amines, diols, aminoalcohols and related compounds. *Tetrahedron: Asymmetry* 1996;7:2687–2694.
- Shapiro MJ, Archinal AE, Jarema MA. Chiral purity determination by proton NMR spectroscopy. Novel use of 1,1'-binaphthyl-2,2'-diylphosphoric acid. *J Org Chem* 1989;54:5826–5828.
- Ravard A, Crooks PA. Chiral purity determination of tobacco alkaloids and nicotine-like compounds by ^1H NMR spectroscopy in the presence of 1,1'-binaphthyl-2,2'-diylphosphoric acid. *Chirality* 1996;8:295–299.
- Lacour J, Hebbe-Viton V. Recent developments in chiral anion mediated asymmetric chemistry. *Chem Soc Rev* 2003;32:373–382.
- Lacour J, Moraleda D. Chiral anion-mediated asymmetric ion pairing chemistry. *Chem Commun* 2009;7073–7089.
- CrysAlis CCD and CrysAlis RED programs, Oxford Diffraction Ltd., Yarnton, Oxfordshire, England, 2010.
- Sheldrick GM. A short history of SHELX. *Acta Crystallogr* 2008;A64:112–122.
- XP. Version 5.1. Bruker AXS Inc., Madison, Wisconsin, USA, 1998.
- Ronwin E. Optical activity and the direct method of acylation. *J Org Chem* 1957;22:1180–1182.
- Pirkle WH, Pochapsky TC. Chiral molecular recognition in small bimolecular systems: a spectroscopic investigation into the nature of diastereomeric complexes. *J Am Chem Soc* 1987;109:5975–5982.
- Gazaliev AM, Balitskii SN, Fazylov SD, Kasenov RZ. Reaction of quinine with dialkyl phosphites in conditions of interphase catalysis. *Zh Obshch Khim* 1991;61:2365–2366.
- Wenzel TJ, Hudson RH. *Discrimination of chiral compounds using NMR spectroscopy*. Hoboken, New Jersey: Wiley; 2007.
- Bürgi T, Baiker A. Conformational behavior of Cinchonidine in different solvents: a combined NMR and ab initio investigation. *J Am Chem Soc* 1998;120:12920–12926.
- Reeder J, Castro PP, Knobler CB, Martinborough E, Owens L, Diederich F. Chiral recognition of *Cinchona* alkaloids at the minor and major grooves of 1,1'-binaphthyl receptors. *J Org Chem* 1994;59:3151–3160.
- Oleksyn BJ, Serda P. Salt-bridge formation by *Cinchona* alkaloids: quinium salicylate monohydrate. *Acta Crystallogr* 1993;B49:530–534.
- Bhatt PM, Ravindra NV, Banerjee R, Desiraju GR. Saccharin as a salt former. Enhanced solubilities of saccharinates of active pharmaceutical ingredients. *Chem Commun* 2005;1073–1075.
- Obaleye JA, Caira MR, Tella AC. Synthesis, characterization and crystal structure of a polymeric zinc(II) complex containing the antimalarial quinine as ligand. *J Chem Crystallogr* 2007;37:707–712.
- Mangwala Kimpende P, Van Meervelt L. Redetermination of Bis{(1S,2S,4S,5R)-2-[(R)-hydroxy(6-methoxy-4-quinolyl)-methyl]-5-vinylquinuclidinium} sulfate dehydrate. *Acta Crystallogr* 2010;E66:2443–2444.